This is the Author's Generated Preprint of an article published in NUCEAR ENGINEERING AND DESIGN and available online at the following link:
https://doi.org/10.1016/j.nucengdes.2015.06.004

HLM Fuel Pin Bundle Experiments in the CIRCE pool facility

Daniele Martelli[1*], Nicola Forgione[1], Ivan Di Piazza[2], Mariano Tarantino[2]

1. University of Pisa, Department of Civil and Industrial Engineering, Pisa, Italy.
2. Italian National Agency for New Technologies, Energy and Sustainable Economic Development, C.R. ENEA Brasimone, Italy.

* Corresponding author. E-mail: daniele.martelli@ing.unipi.it

HIGHLIGHTS

- The experimental results represent the first set of values for LBE pool facility.
- Heat transfer is investigated for a 37-pin electrical bundle cooled by LBE.
- Experimental data are presented toghether with a detailed error analysis.
- Nu is computed as a function of the Pe and compared with correlations.
- Experimental Nu are about 25% lower than Nu derived from correlations.

Abstract

Since Lead-cooled Fast Reactors (LFR) have been conceptualized in the frame of GEN IV International Forum (GIF), great interest has focused on the development and testing of new technologies related to HLM nuclear reactors. In this frame the Integral Circulation Experiment (ICE) test section has been installed into the CIRCE pool facility and suitable experiments have been carried out aiming to fully investigate the heat transfer phenomena in grid spaced fuel pin bundles providing experimental data in support of European fast reactor development. In particular, the fuel pin bundle simulator (FPS) cooled by lead bismuth eutectic (LBE), has been conceived with a thermal power of about 1 MW and a uniform linear power up to 25 kW/m, relevant values for a LFR. It consists of 37 fuel pins (electrically simulated) placed on a hexagonal lattice with a pitch to diameter ratio of 1.8. The FPS was deeply instrumented by several thermocouples. In particular, two sections of the FPS were instrumented in order to evaluate the heat transfer coefficient along the bundle as well as the cladding temperature in different ranks of sub-channels. Nusselt number in the central sub-channel was therefore calculated as a function of the Peclet number and the obtained results were compared to Nusselt numbers obtained from convective heat transfer correlations available in literature on Heavy Liquid Metals (HLM).

Results reported in the present work, represent the first set of experimental data concerning fuel pin bundle behaviour in a heavy liquid metal pool, both in forced and natural circulation. A full characterization of the FPS has been experimentally achieved for Peclet numbers in the range of about 500-3000. Obtained experimental data point out a linear trend of Nusselt number as a function of Peclet in agreement with Mikityuk and Ushakov correlations showing a general tendency to underestimate them; in particular, the newly experimental data points are about 25% lower than Nu derived from correlations available in the literature.

1. Introduction

Within the Generation IV Nuclear reactor international task force (GEN IV International Forum, 2014), the European Commission (European Sustainable Nuclear Industrial Initiatives ESNII) is supporting three GEN IV fast reactor projects (Sodium, Lead and Gas cooled fast reactors) as part of the EU's plan to promote low-carbon energy technologies (SNE-TP, 2013). The sodium-cooled fast neutron reactor technology is actually considered the reference solution (ASTRID project, Le Coz et al. 2011) primarily for Europe's prior experience in sodium technology. Nevertheless, a Lead-cooled fast reactor is the most promising alternative technology for fast reactors. Since lead weakly interact with water or air, the intermediate loop typical of SFR, can be eliminated. Thus, reducing the complexity of the plant and its cost and increasing its safety. Moreover, the LFR showed advantages over the SFR regarding behaviour in severe accidents like ULOF, ULOHS and TLOP (Tuček et al., 2006). Another attractive advantage of the LFR is the low amount of potential (non-nuclear) energy stored in the reactors' primary circuit (twenty times lower than in pressurized water-cooled reactor (PWR) and ten times lower than in sodium coolant respectively, Toshinsky et al., 2013). Potential energy essentially depends from the coolant itself and from operating temperature and pressure, therefore, reactor system such as PWR, LFR and SFR differ by values of potential energy stored in the coolant. As already mentioned lead coolant is chemically inert with air and water hence no chemical energy is stored in the coolant, moreover thanks to the high boiling temperature (about 2016±10 K for lead, see Sobolev, 2007) the pressure can be maintained at atmospheric value (no coolant compression energy stored).

ENEA and the Italian research community are deeply involved in the development of technologies related to Lead-cooled fast reactors for their advances in sustainability, safety, reliability and proliferation-resistance. More in detail, ENEA assumed within the 6^{th} Framework Program EU the commitment to perform an integral experiment aimed at simulating the primary flow path of an LFR pool-type nuclear reactor, implementing a new experimental activity named ICE (Integral Circulation Experiment, Tarantino et al., 2006 and 2011) to be performed in the CIRCE facility (Turroni et al., 2001) where an appropriate test section was installed with the aim of contributing to the demonstration of HLM pool-type reactor feasibility.

Among the planned experimental activities were a series of tests dedicated to the characterization of forced and mixed convection in HLM coolant because heat transfer in HLM significantly differs from the well-known heat transfer in water medium. The leading reason for this changed behaviour lies with the difference in the Prandtl number (Pr) between the two media (Mikityuk, 2009): liquid metals have a relatively low Pr with respect to water ($10^{-2} \div 10^{-3}$ lower than common water). Most of the different experimental work available in HLM scientific literature deals with sodium-potassium alloy (NaK of different composition) or mercury (Hg) as reference fluid (Mikityuk, 2009). Therefore, specific experimental tests with Lead and Lead Bismuth Eutectic alloy (LBE) are mandatory in support of the LFR core thermal-hydraulic design.

This work, deals with the analysis and the discussion of the experimental tests performed with the aim to investigate heat transfer in fuel rod bundles.

The facility test section consists of an electrical bundle (FPS) made up of 37 pins arranged in a hexagonal wrapped lattice with a pitch to diameter ratio of 1.8. Along the FPS active length, two sections were instrumented to monitor the heat transfer coefficient along the bundle as well as the cladding temperatures at different ranks of the sub-channels. The bundle with other components of the ICE test section was placed in CIRCE's large pool experimental facility and natural and forced circulation tests were performed. The Nusselt number in the sub-channels was calculated as a function of the Peclet number and obtained results were compared to the Nusselt number computed from correlations available in the literature.

Symbols

d	Diameter [m]
ΔT	Temperature difference
Hg	Mercury
N	Number of roads
Nu	Nusselt Number [-]
p	pitch [m]
Pe	Peclet Number [-]
Pr	Prandtl Number [-]
Re	Reynolds Number [-]
σ	Standard deviation
X_i	Primary variable
Z	Secondary variable

List of acronyms

ASTRID	Advanced Sodium Technological for Industrial Demonstration
CIRCE	CIRColazione Eutettico
CSC	Central Sub Channel
EC	European Commission
FPS	Fuel Pin bundle Simulator
ENEA	Italian National Agency for New Technologies, Energy and Sustainable Economic Development
ESNII	European Strategic Nuclear Infrastructure Initiative
EU	European Union
FC	Forced Circulation
FPS	Fuel Pin Simulator
GEN-IV	GENeration Four
HLM	Heavy Liquid Metal
ICE	Integral Circulation Experiment
LBE	Lead Bismuth Eutectic alloy
LFR	Lead cooled Fast Reactor
NC	Natural Circulation
OLS	Ordinary Least Squares method
SFR	Sodium Fast Reactor
SNE-TP	Sustainable Nuclear Energy – Technology Platform
TLOP	Total Loss Of Power

ULOF	Unprotected Loss Of Flow
ULOHS	Unprotected Loss Of Heat Sink
Tc	Thermocouple

2. ICE Fuel Pin Simulator

The Integral Circulation Experiment test section (Tarantino et al., 2011) was designed to be implemented in the CIRCE facility (Turroni et al., 2001) aiming at carrying out experimental tests needed to address phenomena related to natural and gas enhanced circulation and to characterize heat transfer in HLM fuel bundles.

The fuel pin simulator, consists of 37 electrical pins placed in a wrapped hexagonal lattice with a pitch-to-diameter ratio (*p/d*) of 1.8, the wrapper edge length is 55.4 mm while the apothem is 48 mm (see Figure 1). The main dimensions of the Fuel Pin Simulator (FPS, Figure 2 (*a*) and (*b*)) of the ICE test section are summarized in Table 1.

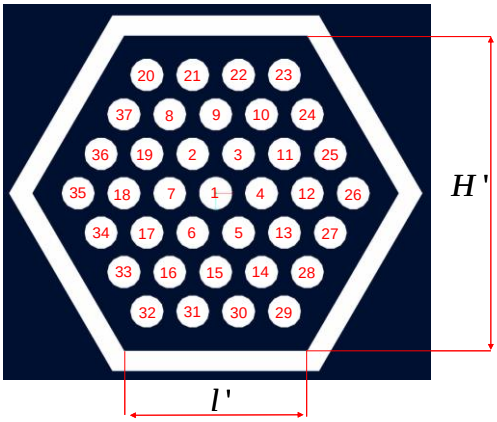

Figure 1: Fuel Bundle geometrical dimensions

Each pin has an outer diameter of 8.2 mm, a linear power of 25 kW/m and a wall heat flux of 1 MW/m^2 (to be considered as maximum values). The nominal thermal power is 800 kW for a total power installed of 925 kW. The active length is 1000 mm, while the cross flow area through the bundle is 6027 mm^2 and the hydraulic diameter of the bundle is about 19 mm (Tarantino et al., 2011). The relative position between the pin bundle and the wrapper is assured by three spacer grids (see Figure 3) appropriately placed along the axis of the component and fixed to the wrapper. The upper and lower spacer grids are placed at the interface between the active and non-active length of the electrical pins to enclose the mixing zones. The middle spacer grid is placed in the middle section of the bundle's active length. From a hydraulic point of view, the wrapper of the FPS assures the overall LBE flow rate runs along the heater bundle, without any by-pass.

(*a*) (*b*)

Figure 2: ICE Fuel Pin Simulator

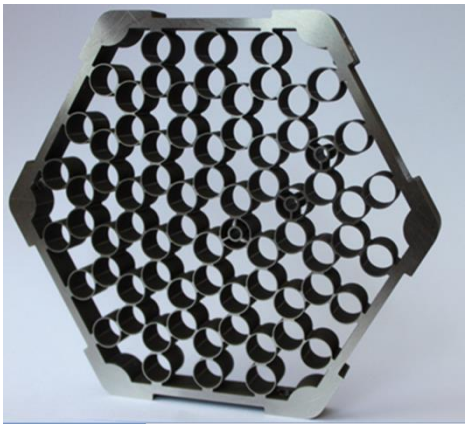

Figure 3: Spacer grid

Table 1: Fuel rod bundle main dimensions

Parameter	Symbol	Value
Number of Pins	*N*	37
Pin outer Parameter	*Φ* [mm]	8.2
Power of a pin	[kW]	25
Pin wall heat flux	[MW/m^2]	1
Pitch-to-diameter ratio	*p/d*	1.8
Pin clad material	-	AISI 316L
Active Length	*L* [mm]	1000
Edge length	*l'* [mm]	55.4
Apothem	*H'/2* [mm]	48

In order to investigate the heat transfer in HLM-cooled rod bundles, the FPS is instrumented with several *N*-type thermocouples having a diameter of 0.5 mm, with an insulated hot junction and an accuracy of ±0.1°C. Regarding the positioning of the thermocouples along the FPS active zone, four different sections are monitored (Figure 4). In this paper, attention is focused on Section 1 and 3, placed 20 mm upstream of the middle spacer grid and 60 mm upstream of the upper spacer grid respectively. In both sections, three different subchannels are instrumented (outer, middle and central subchannel). In each

subchannel, the temperature is monitored at the pins' wall and in the centre of the channel (Figure 5 (*a*) and (*b*)).

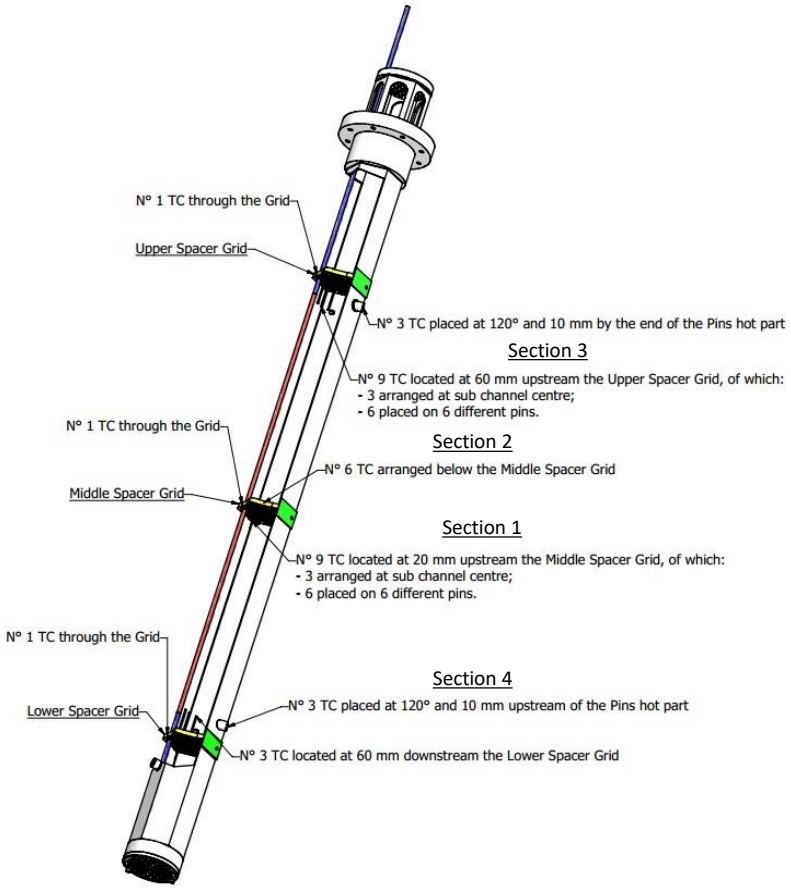

Figure 4: FPS Measurement sections

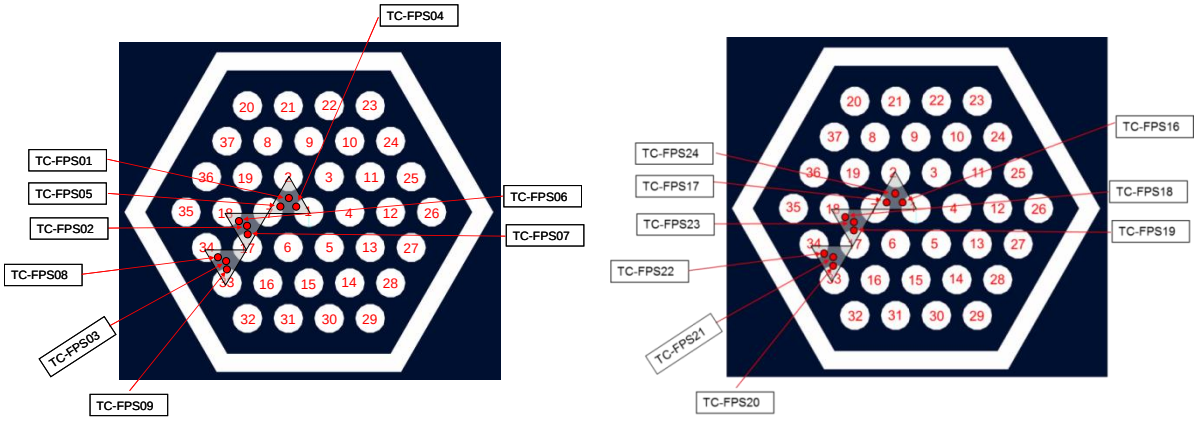

(*a*) (*b*)

Figure 5: Section 1 (*a*) and Section 3 (*b*) instrumentation

In Figure 6 technical solutions adopted for positioning and fixing the thermocouples are shown.

Figure 6: Thermocouples positioning and fixing

Moreover, in order to evaluate the mass flow rate through the ICE test section, a Venturi-nozzle flow meter having an accuracy of 2%, was installed at the entrance of the FPS. Finally, for the calculation of the power supply an accuracy of 1% was considered for both the voltage and current.

3. Experimental procedure

3.1 Experimental Test

The experimental campaign described in this work, was focused on the characterization of heat transfer in a fuel bundle in natural and forced circulation conditions promoted by gas injection (Ambrosini et al., 2005, Benamati et al., 2007). In particular, tests performed in a forced circulation regime were carried out fixing a temperature difference through the FPS of about 80°C and the electrical power to be supplied to the FPS was calculated by an energy balance equation imposing the desired LBE mass flow rate through the FPS. During tests, sub-channel temperatures were investigated at different Peclet numbers, by changing the LBE mass flow rate in the range of 40-70 kg in steps of about 5 kg/s. For each step, steady state temperature conditions in the FPS were reached and maintained at least for 15 min and the Nusselt number was evaluated.

The adopted boundary conditions are summarized in Table 2. In particular, the imposed LBE mass flow rate, the FPS electrical power to obtain the desired difference in temperature between the FPS inlet and outlet section are reported. Moreover, the difference between the pin clad temperature and the sub-channel bulk temperature, foreseen using the Mikityuk and Ushakov correlations for the Nu evaluation are reported (Mikityuk, 2009 and Ushakov et al., 1977). All data reported in the paper refers to the central subchannel of the FPS and a reasonable approximation is to consider the central subchannel as being representative of an infinite lattice.

Table 2: Boundary conditions adopted for FC tests

Name	LBE Mass flow rate [kg/s]	FPS Electrical Power [kW]	ΔT (outlet-inlet) FPS [°C]	ΔT (clad-bulk) Mikityuk [°C]	ΔT (clad-bulk) Ushakov [°C]
1-FC	70	800	80	35.0	36.0
2-FC	65	760	80	37.0	39.0
3-FC	60	700	80	39.5	41.0
4-FC	55	640	80	41.6	43.5
5-FC	50	580	80	43.5	45.7
6-FC	45	525	80	45.4	47.8
7-FC	40	465	80	47.0	49.5

For tests performed in natural circulation conditions, the power supplied to the FPS was changed from 100 to 600 kW in steps of 100 kW, obtaining LBE flow rate through the test section in the range of 12-25 kg/s. For each step, steady state temperature conditions in the FPS were reached and maintained for at least 15 mins. In Table 3 a short description of natural circulation tests is reported; in particular, the electrical power supplied to the FPS and the obtained LBE flow rate are summarized.

Table 3: NC tests description

Name	LBE Mass flow rate [kg/s]	FPS Electrical Power [kW]
1-NC	25	600
2-NC	23	500
3-NC	21	400
4-NC	19	300
5-NC	14	200
6-NC	12	100

Thermocouples mounted on the pin wall, are kept in place by a thin metal sheet welded on the pin clad. Furthermore, an additional correction for the wall temperature is required to take into account the position of the thermocouple fixed to the pin external wall with an AISI 304 sheet. The wall temperature value obtained considering the correction to account for the thermal conduction phenomena is given by:

$$T_{W,corr} = T_{W,\exp} + \frac{\dot{Q}}{N\pi D_{pin} L_{heat}} \cdot \frac{D_{TC}/2}{k_{AISI\,304}} \tag{1}$$

where D_{TC} is the diameter of the thermocouple and L_{heat} is the active pin length and $\dot{Q}$ is the thermal power supplied to the FPS. The heat transfer coefficient is calculated by the Newton relationship $HTC=q''/(T_{wall}-T_b)$, where q'' is the heat flux obtained from an energy balance in order to account heat losses from the FPS wrapper to the surrounding LBE in the pool, T_{wall} and T_b are the clad and the coolant bulk temperatures respectively. The bulk temperature on the middle and upper Sections (1 and 3) are obtained considering a linear trend between the average temperature values at the entrance and at the exit of FPS active length.

3.2 Uncertainty analysis

In this work, sources of error in the performed measurements are considered and the effect of the uncertainty in single measurement on the calculated results is investigated (Lichten, 1999 and Moffat, 1988). In particular, assuming a quantity Z (secondary variable) computed using a set of independent experimental measurements X_i (primary variables) can be represented as $Z=Z(X_1, X_2.. X_n)$. The uncertainty in the calculated results can be estimated with good accuracy using a root-sum square combination of the effect of uncertainties of each individual input X_i:

$$\sigma_Z = \sqrt{\left(\frac{\partial Z}{\partial X_1}\right)^2 \sigma_{x_1}^2 + .. + \left(\frac{\partial Z}{\partial X_n}\right)^2 \sigma_{x_n}^2} \tag{2}$$

where σ_{X_i} is the standard deviation given by:

$$\hat{\sigma}_{X_i} = \sqrt{\frac{\sum_{1}^{t}(X_i(t) - \overline{X_i})^2}{t-1}} \tag{3}$$

For each of the primary variables, global uncertainty is considered composed by the instrument uncertainty and the standard deviation of the considered variable X_i according to:

$$\sigma^2_{X_i} = \hat{\sigma}^2_{X_i} + \sigma^2_{X_i,\,Instr.} \tag{4}$$

The primary variables experimentally measured in this work are temperatures and LBE mass flow rate. Regarding the coolant properties, all the empirical correlations used in this work, are in agreement with the correlation for Lead-bismuth Eutectic available in the Handbook on Lead-bismuth Eutectic alloy, 2007 and their own accuracy is considered.

In order to obtain a standard deviation representative of the dispersion and neglecting effects due to an imperfect stationary of acquired experimental variables, a linear regression for each of gained thermocouple signals was evaluated and subtracted from the original one. In particular, linear regression was computed using the Ordinary Least Squares method (OLS). The statistical standard deviation was finally calculated using the modified data.

Figure 7 (*a*), shows temperature data in the centre of the channel and its linear regression for Test 1-FC; after 15 min the temperature decreases by about 1°C. Figure 7 (*b*) shows the modified temperature values obtained reducing the modified source signal by its linear regression.

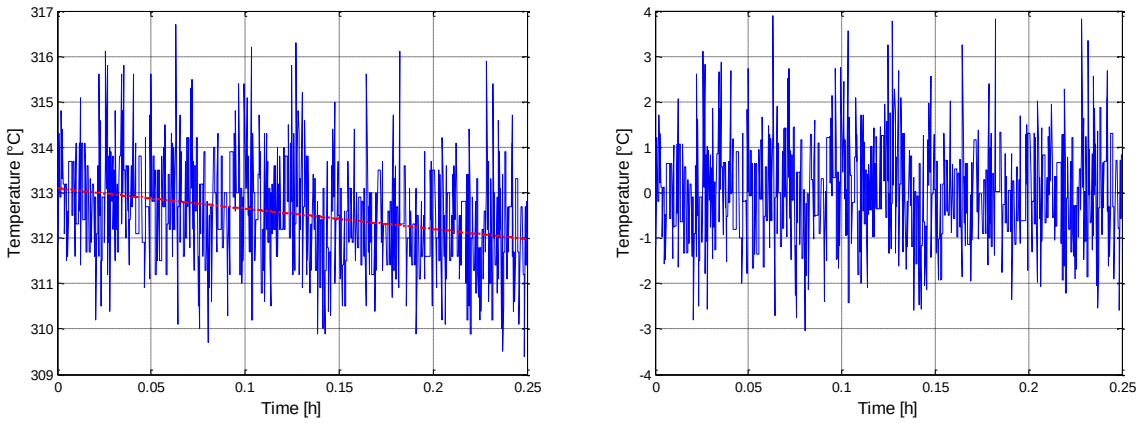

(*a*) **(*b*)**

Figure 7: Test 1-FC, temperature in the centre of the channel (*a*) and modified signal for statistical calculations (*b*)

It must be noticed that for the purpose of Nu calculations, stationary conditions must be guaranteed for the temperature difference between the wall and the bulk.

4. Experimental Results

For Test 1-FC the temperature difference between the inlet and outlet section of the FPS obtained for setting the electrical power supplied to the bundle of 800 kW is 77°C (Figure 8 (*a*)), about 7°C lower than the temperature set in the calculation of the required electrical power (see Table 2). The

injection of Argon gas (5 Nl/s) ensured an averaged LBE mass flow rate through the FPS of about 70 kg/s (Figure 8 (*b*)).

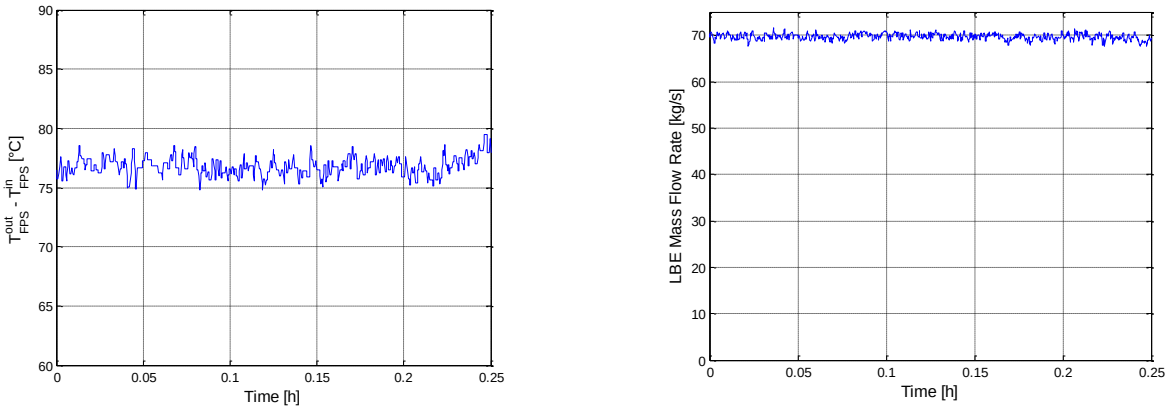

(*a*) (*b*)

Figure 8: Test 1-FC, Δ*T* trough the FPS (*a*) and LBE mass flow rate (*b*)

Temperatures monitored in the central subchannel of Section 1 (see Figure 5 (*a*)) are plotted in Figure 9 (*a*). The experimental temperature measured on pins 1 and 7 is about 366°C while the temperature in the centre of the channel is 312°C, i.e. about 54°C lower that the pin temperature and about 19°C higher than temperature foreseen using Mikityuk and Ushakov correlations (see Table 1). The average velocity in the FPS (both Section 1 and 3) is about 1.1 m/s and the Peclet number is about 2933 at Section 1. Considering the central subchannel of Section 1, the wall temperature is obtained averaging temperatures measured on the walls of pin 1 and pin 7; moreover, this value is corrected according Eq. (1) in order to take into account the position of the thermocouple fixed to the pin external wall with an AISI 304 sheet. The wall temperature thus calculated is 377.2°C, about 11°C higher than the measured value reported in Figure 9 (a). The bulk temperature in the central subchannel at Section 1, obtained considering a linear trend between the average temperature values at the entrance and at the exit of FPS active length, is 362.8°C about 10°C higher than the temperature measured in the centre of the channel. The Nusselt number calculated for the central subchannel and reported in Figure 9 (*b*) is 26.3.

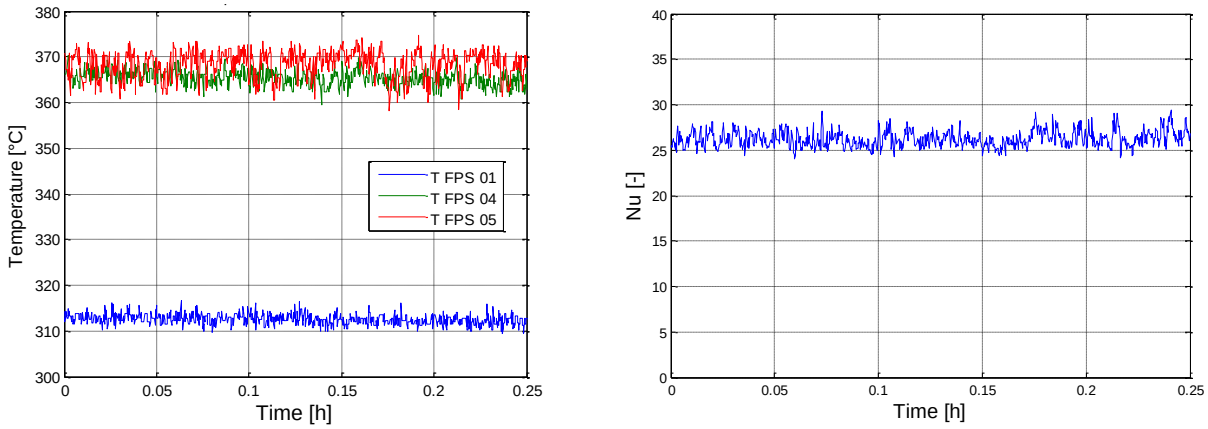

(*a*) (*b*)

Figure 9: Section 1, central sub-channel temperatures (a) and Nusselt number (b)

Considering the central subchannel of Section 3 (see Figure 5 (*b*)) the average temperature in the centre of the channel is about 355°C about 4°C lower than the bulk temperature while the average temperature measured on pin 1 is about 412°C. The average temperature measured on pin 7 is 395°C, about 17°C lower than on Pin 1.

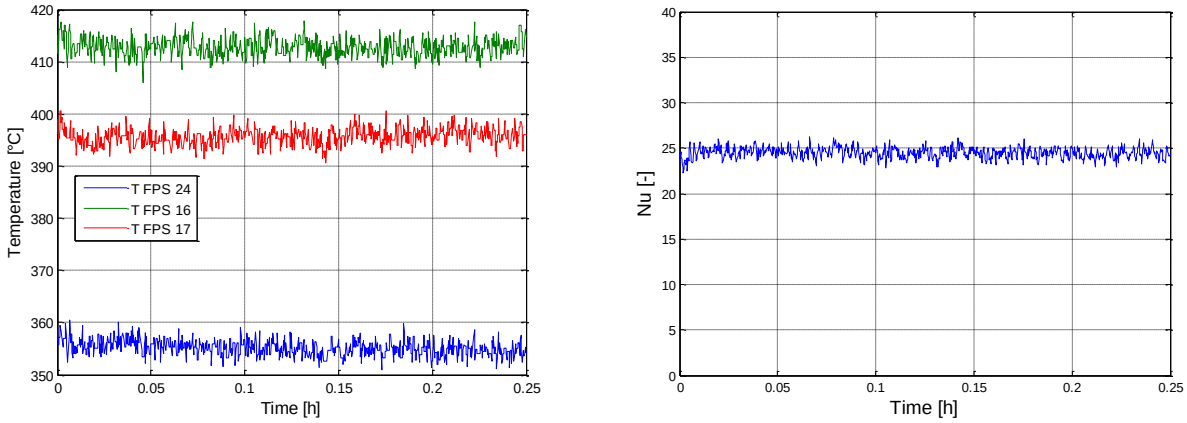

(*a*) (*b*)

Figure 10: Section 3, central sub-channel temperatures (a) and Nusselt number (b)

This difference is essentially caused by pin manufacturing as reported in Figure 11. Due to the internal geometry adopted for Bifilar-type pins, provided by Thermocoax, the heat flux around a pin is not uniform. From Thermocoax technical documents, bifilar-type pin rods used in the ICE bundle, exhibit an approximate azimuthal variation $\left(q''_{\max} - q''_{\min}\right)/\overline{q''} \approx 0.3$ of about 30% (±15%, Bandini et al., 2011); therefore, the temperatures measured by the wall-pinched thermocouples can differ from the average wall temperatures. This will be taken into account later, in the error measurement analysis for the correction of the wall temperature and in the temperature difference between T_w and T_b. The wall temperature corrected as reported in Eq. (1) is 414.2°C about 10°C higher than the mean of the experimental data. The averaged Nusselt number calculated for the Section 3 in the central subchannel is 24.5 (Figure 10 (*b*)).

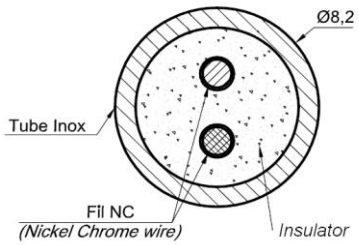

Figure 11: Cross section of the Bifilar-type pin (active zone)

Considering Test 1-NC performed in natural circulation conditions the temperature difference between the inlet and outlet sections of the FPS, obtained by setting the electrical power supplied to the bundle at 600 kW, is about 174°C (Figure 12 (*a*)). Regarding the operation in natural circulation regime the difference in level (*H*) between the thermal centre of the heat source (FPS) and the one of the heat sink

(Heat Exchanger, HX) provides the pressure head ($\Delta p \sim g\beta\Delta T\Delta H$) required to guarantee the LBE mass flow rate. The obtained LBE mass flow rate shown in Figure 12 (*b*) for Test 1-NC is about 25 kg/s.

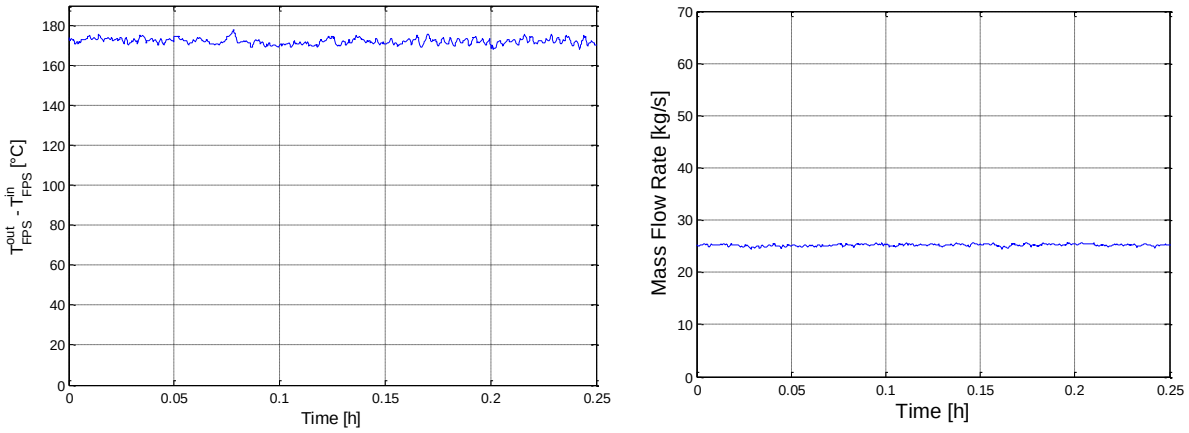

(***a***) (***b***)

Figure 12: Test 1-NC, *ΔT* trough the FPS (*a*) and LBE mass flow rate (*b*)

The average temperature measured on pin 1 and 7 at Section 1 is about 434°C while the average temperature in the centre of the channel is about 372°C and the temperature difference pin-centre channel is about 62°C (see Figure 13 (*a*)). The pin wall temperature corrected according to Eq.1 is 441.4°C while the bulk temperature is about 388°C. The averaged velocity in the bundle is 0.41 m/s and the obtained Nusselt number is 20.3. In the upper section (Section 3) the average experimental temperature measured on the pin 1 is about 522°C (Figure 14 (*a*)) while on pin 7 it is about 11°C lower than on pin 1 due to the azimuthal variation of the thermal flux around the bifilar-type pin rods. The corrected pin wall temperature is about 524°C while the bulk temperature is 468.1°C. The obtained Nu number for Test 1-NC at Section 3, shown in Figure 14 (*b*), is 18.0.

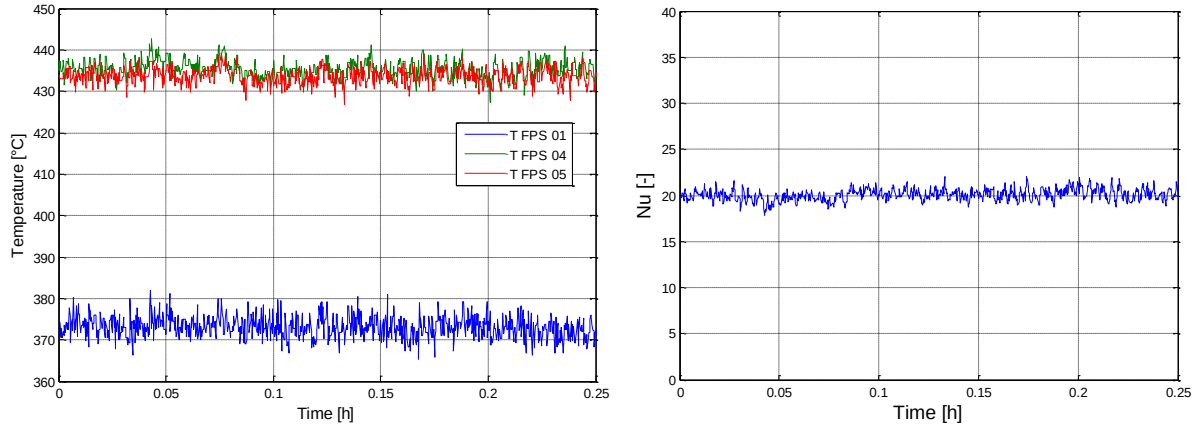

(***a***) (***b***)

Figure 13: Section 1, central sub-channel temperatures (a) and Nusselt number (b)

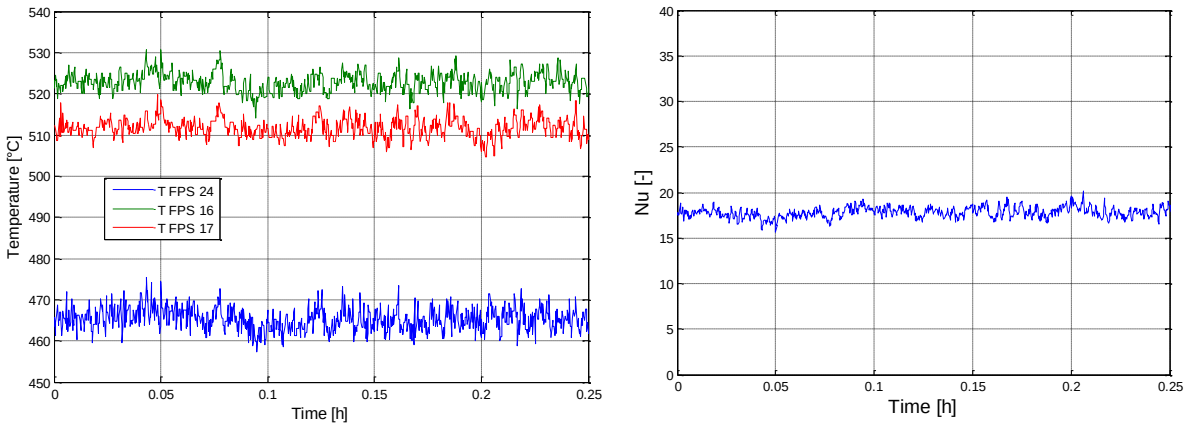

(*a*) **(*b*)**

Figure 14: Section 3, central sub-channel temperatures (a) and Nusselt number (b)

The main experimental primary variables for tests performed both in forced and natural circulation are summarized in Table 4 and Table 5. In particular, the LBE mass flow rate flowing through the bundle is reported together with temperatures in the centre of the channel and on the considered pin (Pin 1 and 7) for Section 1 (Table 4) and Section 3 (Table 5). Moreover, the standard deviation and the percentage error is reported for each variable in agreement with § 3.2. In Table 4 are also reported the average temperatures at the inlet and outlet sections of the FPS.

In forced circulation conditions, reducing the argon flow rate, the gas bubble flow was not uniform leading to an increase in mass flow rate dispersion of the measured data and, therefore, to an increase of the spread in temperature data in the bundle. For this reason LBE mass flow rate values lower than about 40 kg/s could not be reached in forced circulation conditions. On the other hand, the maximum LBE mass flow rate reached in natural circulation conditions without an excessive increase of the pin wall temperature is about 25 kg/s.

Table 4: Primary variables measured at Section 1 and their uncertainties

Name	$\overline{\dot{m}}$ [kg/s]	$\langle\sigma_X\rangle$ [kg/s]	$\left\langle\frac{\sigma_X}{X}\right\rangle$	$\overline{T}_{CC}$ [°C]	$\langle\sigma_X\rangle$ [°C]	$\overline{T}_{Pin1}$ [°C]	$\langle\sigma_X\rangle$ [°C]	$\overline{T}_{Pin7}$ [°C]	$\langle\sigma_X\rangle$ [°C]	$\overline{T}^{in}_{FPS}$ [°C]	$\langle\sigma_X\rangle$ [°C]	$\overline{T}^{out}_{FPS}$ [°C]	$\langle\sigma_X\rangle$ [°C]
1-FC	69.7	1.5	2.2%	312.5	1.1	365.4	1.6	368.30	3.0	286.0	0.8	362.8	1.4
2-FC	65.7	1.5	2.3%	311.1	1.1	362.6	1.5	363.70	2.8	283.7	1.1	360.8	1.6
3-FC	60.1	1.5	2.5%	300.5	1.2	351.2	1.7	348.70	2.3	272.5	0.9	350.8	2.0
4-FC	55.4	1.4	2.5%	304.2	1.3	351.9	1.9	351.70	2.0	274.9	1.1	351.9	2.0
5-FC	49.4	1.9	3.8%	297.9	1.8	343.2	2.7	342.20	2.6	268.6	1.2	346.8	3.0
6-FC	43.8	2.6	5.9%	291.1	2.6	335.8	3.7	335.00	3.8	260.3	1.3	342.1	4.3
7-FC	40.6	2.8	6.9%	285.1	2.7	325.4	4.2	324.60	4.0	255.2	1.1	333.8	4.7
1-NC	25.2	0.5	2.0%	372.4	2.5	435.0	2.1	433.10	2.0	304.6	1.3	478.5	2.2
2-NC	23.2	0.5	2.2%	375.9	2.3	428.6	1.9	427.60	1.7	313.8	1.4	471.2	2.1
3-NC	21.1	0.5	2.4%	409.3	1.7	452.3	1.3	450.40	1.4	351.1	0.8	488.9	2.1
4-NC	19.2	0.4	2.1%	398.6	1.4	431.2	1.1	429.70	1.1	349.4	0.9	463.2	1.5
5-NC	14.1	0.3	2.1%	341.0	1.5	364.2	1.2	364.40	1.2	295	1.9	400.9	3.1
6-NC	12.7	0.3	2.4%	309.2	0.8	321.1	0.7	321.80	0.8	282.1	0.8	341.9	1.7

Table 5: Primary variables measured at Section 3 and their uncertainties

Name	$\overline{\dot{m}}$ [kg/s]	$\langle\sigma_X\rangle$ [kg/s]	$\left\langle\frac{\sigma_X}{X}\right\rangle$	$\overline{T}_{CC}$ [°C]	$\langle\sigma_X\rangle$ [°C]	$\overline{T}_{Pin1}$ [°C]	$\langle\sigma_X\rangle$ [°C]	$\overline{T}_{Pin7}$ [°C]	$\langle\sigma_X\rangle$ [°C]
1-FC	69.7	1.5	2.2%	355.1	1.4	412.8	1.7	395.6	1.6
2-FC	65.7	1.5	2.3%	352.7	1.6	409.9	1.7	393.8	1.6
3-FC	60.1	1.5	2.5%	342.9	1.9	397.8	2.0	383.0	2.0
4-FC	55.4	1.4	2.5%	348.0	2.1	398.6	2.2	384.7	2.2
5-FC	49.4	1.9	3.8%	339.8	3.3	387.3	3.9	378.2	4.1
6-FC	43.8	2.6	5.9%	334.8	5.1	380.7	6.1	372.5	6.2
7-FC	40.6	2.8	6.9%	325.9	5.5	368.9	7.0	361.4	6.6
1-NC	25.2	0.5	2.0%	464.8	2.7	522.4	2.4	511.3	2.3
2-NC	23.2	0.5	2.2%	460.5	2.4	509.6	2.0	498.8	1.7
3-NC	21.1	0.5	2.4%	482.7	2.1	522.1	1.7	514.1	1.6
4-NC	19.2	0.4	2.1%	459.4	1.7	490.3	1.4	486.8	1.4
5-NC	14.1	0.3	2.1%	397.8	1.9	420.7	1.6	417.9	1.5
6-NC	12.7	0.3	2.4%	341.8	1.2	353.6	0.9	352.7	0.9

The Nu number was then calculated considering the equivalent diameter as the characteristic length, which is, for a triangular interior channel (assuming an infinite lattice), evaluated by:

$$d_{eq} = 4\frac{\left(\frac{\sqrt{3}}{4}\cdot p^2 - \pi\cdot d\right)}{\frac{\pi\cdot d}{2}} \tag{5}$$

In Table 6 the Nu numbers computed for all the performed experimental Tests are reported together with the Pe and Re numbers. These variables are secondary variables hence the propagation of errors are calculated, as discussed in § 3.2, taking the root-sum-of-squares of all partial error to get the total error (Moffat, 1988).

Table 6: Secondary variables at Section 1 and their uncertainties

Name	Re	$\langle\sigma_x\rangle$	$\left\langle\frac{\sigma_x}{X}\right\rangle$	Pe	$\langle\sigma_x\rangle$	$\left\langle\frac{\sigma_x}{X}\right\rangle$	Nu	$\langle\sigma_x\rangle$	$\left\langle\frac{\sigma_x}{X}\right\rangle$
1-FC	$1.4\ 10^5$	$7.8\ 10^3$	5.6%	2933	263	9%	26.3	2.6	10.0%
2-FC	$1.3\ 10^5$	$7.4\ 10^3$	5.7%	2772	249	9%	25.8	2.6	10.1%
3-FC	$1.2\ 10^5$	$7.0\ 10^3$	6.0%	2572	237	9%	26.0	2.7	10.4%
4-FC	$1.1\ 10^5$	$6.5\ 10^3$	6.0%	2365	218	9%	23.9	2.5	10.5%
5-FC	$9.5\ 10^4$	$6.8\ 10^3$	7.1%	2122	212	10%	23.8	2.9	12.3%
6-FC	$8.3\ 10^4$	$7.5\ 10^3$	9.0%	1896	217	11%	23.0	3.5	15.3%
7-FC	$7.6\ 10^4$	$7.4\ 10^3$	9.7%	1776	213	12%	23.2	3.8	16.6%
1-NC	$5.\ 710^4$	$3.1\ 10^3$	5.5%	984	88	9%	20.3	2.1	10.1%
2-NC	$5.2\ 10^4$	$3.0\ 10^3$	5.7%	903	82	9%	20.0	2.1	10.3%
3-NC	$5.0\ 10^4$	$2.8\ 10^3$	5.6%	796	71	9%	17.8	1.8	10.2%
4-NC	$4.5\ 10^4$	$2.5\ 10^3$	5.6%	738	66	9%	17.7	1.7	9.9%
5-NC	$3.0\ 10^4$	$1.7\ 10^3$	5.7%	579	52	9%	18.8	3.2	16.9%
6-NC	$2.5\ 10^4$	$1.4\ 10^3$	5.8%	542	49	9%	17.2	2.3	13.2%

Table 7: Secondary variables at Section 3 and their uncertainties

Name	Re	$\langle\sigma_x\rangle$	$\left\langle\frac{\sigma_x}{X}\right\rangle$	Pe	$\langle\sigma_x\rangle$	$\left\langle\frac{\sigma_x}{X}\right\rangle$	Nu	$\langle\sigma_x\rangle$	$\left\langle\frac{\sigma_x}{X}\right\rangle$
1-FC	$1.5\ 10^5$	$8.4\ 10^3$	5.6%	2812	252	9%	24.5	2.3	9.3%
2-FC	$1.4\ 10^5$	$8.0\ 10^3$	5.7%	2657	239	9%	23.6	2.2	9.4%
3-FC	$1.3\ 10^5$	$7.6\ 10^3$	6.0%	2462	227	9%	23.0	2.3	9.8%
4-FC	$1.2\ 10^5$	$7.0\ 10^3$	6.0%	2266	209	9%	21.2	2.1	9.9%
5-FC	$1.0\ 10^5$	$7.4\ 10^3$	7.1%	2031	203	10%	21.1	2.4	11.4%
6-FC	$9.0\ 10^4$	$8.1\ 10^3$	9.0%	1811	207	11%	20.7	3.0	14.4%
7-FC	$8.2\ 10^4$	$8.0\ 10^3$	9.7%	1698	204	12%	20.6	3.3	16.0%
1-NC	$6.4\ 10^4$	$3.6\ 10^3$	5.5%	903	80	9%	18.0	1.8	9.8%
2-NC	$5.9\ 10^4$	$3.4\ 10^3$	5.7%	835	76	9%	17.4	1.7	9.9%
3-NC	$5.5\ 10^4$	$3.1\ 10^3$	5.6%	745	67	9%	15.5	1.4	9.3%
4-NC	$4.8\ 10^4$	$2.7\ 10^3$	5.6%	698	63	9%	14.3	1.4	9.7%
5-NC	$3.2\ 10^4$	$1.9\ 10^3$	5.7%	548	50	9%	13.7	1.9	13.9%
6-NC	$2.6\ 10^4$	$1.5\ 10^3$	5.8%	524	48	9%	12.5	1.6	12.9%

Figure 15 shows the Nu number computed from the experimental data as a function of the Pe number and a comparison with correlations available in the literature (Mikityuk, 2009, Pfrang and Struwe, 2007).

In particular, among correlations for circular rods arranged in a triangular lattice, we selected two of them, Mikityuk and Ushakov correlations (Mikityuk, 2009 and Ushakov et al., 1977), with a validity range containing the *p*/*d* ratio used for the CIRCE-ICE experimental campaign. Mikityuk correlation is here reported:

$$Nu = 0.047 \cdot \left(1 - e^{-3.8 \cdot (x-1)}\right)\left(Pe^{0.77} + 250\right) \qquad (6)$$

valid for $1.1 \le p/d \le 1.95$ and for $30 \le Pe \le 5000$

It gives the best fit of four set of experimental data (658 data points). It is obtained from the review of experimental results obtained by Maresca and Dwyer, 1964, Borishanskii et al., 1969, Gräber and Rieger, 1972 and Zhukow et al., 2002 available in the literature. Mikityuk correlation is recommended for square and triangular lattice of rods with *p*/*d* ratio of 1.1-1.95 and Peclet numbers up to 5000, it must be stressed, however, that correlations have an uncertainty due to the heterogeneity of the original data and moreover they are derived for different heavy metals.

The Ushakov correlation (Eq. (7)), is found by Mikityuk (2009) to have the highest quality in predicting the experimental data considered in the paper (no direct access to Ushakov's reference was available, however the discussion of this correlation was found documented in A.V. Zhukov et al., 1992). The validity range is for Pe up to 4000 and *p*/*d* in the range 1.2-2.

$$Nu = 7.55 \cdot \left(p/d\right) - 20 \cdot \left(p/d\right) + 0.041 \cdot \left(p/d\right)^{-2} \cdot Pe^{\left(0.56 + 0.19 \cdot p/d\right)} \qquad (7)$$

valid for $1.2 \le p/d \le 2$ and for $1 \le Pe \le 4000$

The experimental results show a linear trend in agreement with data obtained from the correlations of Ushakov and Mikityuk and a general trend to lie below Nu values obtained from them. Differences between Section 1 and Section 3 in the experimental data are supposed to be generated by the fact that Section 1 is nearest to the spacer grid with respect to Section 3, hence, the heat transfer is most affected by the turbulence increased by the grid itself.

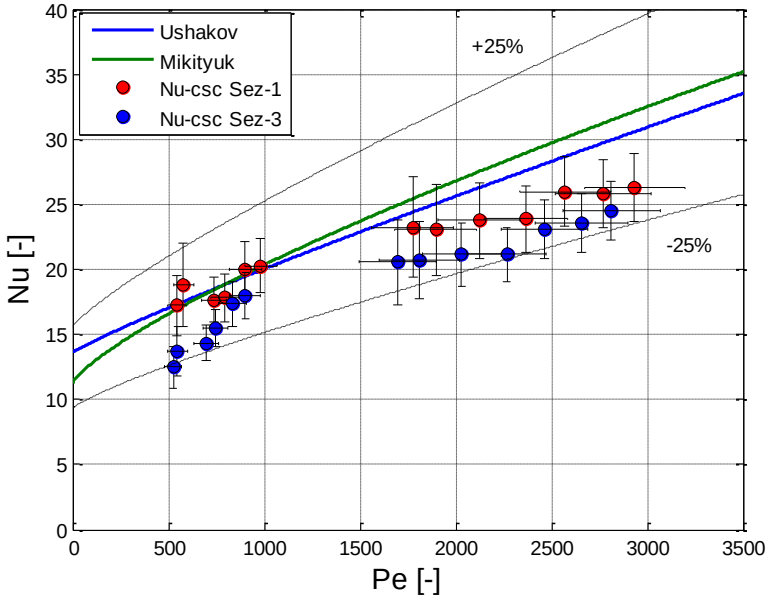

Figure 15: Experimental Nu vs. Pe number and comparison with Mikityuk and Ushakov correlations

5. Conclusions

This work describes the experimental activity carried out at the ENEA Brasimone Research Centre dealing with the analysis of heat transfer in a 37-pin fuel rod bundle cooled with LBE under typical large pool reactor conditions.

A detailed description of the ICE Test section is presented and the instrumentation of the bundle is reported.

Then an extended characterization of the performed experiments is introduced and differences between the operation of natural and forced circulation tests are shown.

In order to obtain a standard deviation representative of the dispersion and neglecting effects due to an imperfect stationary of acquired experimental variables, a linear regression for each gained thermocouple signal was evaluated and subtracted from the original one. In particular, linear regression was computed using the Ordinary Least Squares method (OLS). The statistical standard deviation was finally calculated using the modified data and the accuracy of the instrumentation.

For each of the performed experiments (seven tests operated in forced circulation and six in natural circulation conditions) Nusselt numbers were evaluated within a Peclet range of 500-3000.

The uncertainty of the obtained Nu is within ±20%, while the uncertainty of the Pe is within ±12%.

The central copper pin rod solution was not adopted because of manufactory problems related to the required length to reach the downcomer of the CIRCE pool main vessel (about 8 m).

The Nu experimental data were then compared with values obtained from correlations available in literature for heat transfer convection in heavy liquid metals. In particular, a comparison with data obtained from Mikityuk and Ushakov correlations is presented.

Experimental data point out a linear trend in agreement with the above-cited correlations; in particular, the experimental Nu values differ from Nu obtained by Mikityuk and Ushakov correlations by less than 25%.

Finally, the results reported in the present work relate to the CIRCE-ICE experiments and represent the first set of experimental data concerning fuel pin bundle behaviour in a heavy liquid metal pool, both in forced and natural circulation. Future and innovative nuclear systems based on the HLM technologies (ADSs, LFRs) will be supported by these experiments in their design, safety analysis and licensing phases.

Acknowledgements

The authors gratefully acknowledge the work done by the staff of the thermal-fluid-dynamic and facility operation laboratory of the experimental engineering technical unit of Brasimone (UTIS-TCI) for the operation of CIRCE facility.